Comparison of Two Coaxial Probes for Measuring the Steel Fiber Content in Fiber Reinforced Concrete Slabs

S. Van Damme* A. Franchois* P. De Pauw† L. Taerwe†

Abstract — **Recently, a non-destructive measuring technique to measure the steel fiber content in steel fiber reinforced concrete was proposed by the authors. The technique is based on permittivity measurements using an open-ended coaxial probe. In previous work, a moderate sized probe was used. From the results using this probe, the need for a larger probe was clear. In this paper, measurements using an in-house designed large probe are compared with the measurements from the moderate sized probe.**

1 INTRODUCTION

In steel fiber reinforced concrete (SFRC), steel fibers are randomly added to the concrete, yielding a better tensile strength. This type of reinforcement is used more and more in applications such as slabs on grade and pavements. An important quality aspect is the uniform spatial distribution of the fibers throughout the concrete. Locations with lower fiber contents have a lower strength. The fibers also should have a random orientation to withstand tensile forces in different directions. Today, the fiber content in SFRC slabs is checked in a destructive manner by drilling out a core, crushing it and counting the number of fibers [1]. This technique has a lot of drawbacks. Recently, we developed a non-destructive technique based on the use of microwaves [2]. It combines an accurate open-ended coaxial probe reflectometry method, in order to measure the effective permittivity of the reinforced concrete, with a classical mixing formula, which establishes the relationship between the effective permittivity and the fiber content. Measurements performed with a moderate sized probe on SFRC slabs showed important local spatial fluctuations in the permittivity. This was probably due to the limited size of the probe aperture with respect to the dimensions of the fibers. Therefore, a spatial averaging of the measurements was introduced to improve the homogenization. In this paper we have built a larger probe. It is shown that with this probe spatially stable results can be obtained.

In Section 2 a Maxwell-Garnet mixing rule is given for SFRC. In section 3, the open-ended coaxial probe method is described. Results obtained with the moderate sized probe are shortly discussed in section 4 and in section 5 measurements with the large probe are reported. In section 6 the results from both probes are compared.

2 MIXING RULE FOR STEEL FIBER REINFORCED CONCRETE

Concrete is made by mixing cement, water, fine and coarse aggregates. After the mixing, the concrete hardens as a result of a chemical reaction between water and cement. Steel fibers can be added to the fresh concrete as reinforcement. The amount of steel fibers depends on the type of fiber and on the required strength and is typically in the range of 20 kg/m^3 to 80 kg/m^3, which corresponds to sparse mixtures with volume fractions between 0.002 and 0.01. The length l and diameter d of the fiber are in the ranges 10 mm $< l <$ 80 mm and 0.1 mm $< d <$ 1 mm.

Concrete and SFRC are heterogeneous materials, but for wavelengths that are large compared to the dimensions of the composing particles, they can be considered as homogeneous. In this case, homogenization theories can be applied. In this paper SFRC is considered as a homogeneous concrete backgound material with relative permittivity $\varepsilon_{\mathrm{r,h}}$ containing a volume fraction f_{v} of perfectly electrically conducting prolate spheroids. In [2], a Maxwell-Garnett mixing formula was derived, giving the relationship between the real part of the relative effective permittivity $\varepsilon'_{\mathrm{r,eff}}$ of SFRC and the fiber volume fraction:

$$\varepsilon'_{\mathrm{r,eff}} = \varepsilon'_{\mathrm{r,h}} \left[1 + \frac{f_{\mathrm{v}}}{3(1-f_{\mathrm{v}})} \sum_{i=1}^{3} \frac{1}{N_{\mathrm{i}}} \right], \qquad (1)$$

where $N_{\mathrm{i}}, i = 1, 2, 3$, are the depolarization factors of an ellipsoid. From (1) it is clear that for small volume fractions, as used in this work, the relative

*Dept. of Information Technology (INTEC-IMEC), Ghent University, St. Pietersnieuwstraat 41, 9000 Gent, Belgium, e-mail: stephan.van.damme@intec.ugent.be, tel.: +32 (0)9 2649995, fax: +32 (0)9 2649969; e-mail: ann.franchois@intec.ugent.be

†Dept. of Structural Engineering, Ghent University, Technologiepark Zwijnaarde 904, 9052 Gent, Belgium, e-mail: Peter.DePauw@ugent.be, tel.: +32 (0)9 2645530, fax: +32 (0)9 2645845; e-mail: Luc.Taerwe@ugent.be

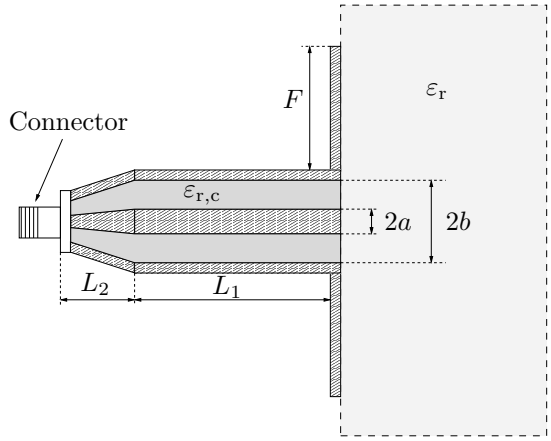

Figure 1: Open-ended coaxial probe configuration.

permittivity contrast $(\varepsilon'_{r,eff} - \varepsilon'_{r,h})/\varepsilon'_{r,h}$ depends linearly on the fiber volume fraction.

3 OPEN-ENDED COAXIAL PROBE METHOD

The open-ended coaxial probe as a tool to measure the relative complex permittivity $\varepsilon_r = \varepsilon'_r - j\varepsilon_r$" at microwave frequencies has been studied intensively in the literature, e.g. [3]-[6]. The probe is schematically presented in Fig. 1. The inner and outer conductors have radii a and b, respectively, and the space between both conductors is filled with a material with relative permittivity $\varepsilon_{r,c}$. The lengths of the straight and tapered sections are L_1 and L_2, respectively. A flange with dimension F, extending the outer conductor, allows to establish a stable contact with the slab and it makes the electromagnetic modelling of the probe easier.

The relative complex permittivity can be derived from the TEM-mode reflection coefficient at the probe aperture by using an appropriate model for the aperture input admittance. In this paper two full-wave models, that account in an exact way for the evanescent higher order TM_{0n} modes at the probe aperture, are applied. Both models are based on the assumption of a flange of infinite extent, which in practice is fulfilled if $F > b$. The first model is the rational function approximation proposed by Stuchly *et al.* [4]. This model is valid for the class of 50 Ω Teflon-filled probes applied against a (possibly lossy) dielectric half-space and is computationally very efficient. The second model, proposed by De Langhe *et al.* [3], is computationally more intensive, but it can be used in case of a one-dimensional layered medium, e.g. to account for the finite thickness of a slab.

4 MEASUREMENTS WITH A MODERATE SIZED PROBE

This is a 50 Ω Teflon-filled probe with the following parameters (Fig. 1): $a = 5.9$ mm, $b = 20$ mm, $F = 60$ mm, $L_1 = 95$ mm, $L_2 = 30$ mm and $\varepsilon_{r,c} = 2.1$. It is shown in Fig. 2, together with rest of the measurement setup (a flexible test-port cable, an Agilent 8714ET Vector Network Analyzer and a PC). This probe was used for the measurements reported in [2], that were performed on three different concrete slabs with dimensions 600 mm x 600 mm x 100 mm: slab S00 without fibers ($f_v = 0$), slab S20 with 20 kg/m^3 of fibers ($f_v = 0.0024$) and slab S40 with 40 kg/m^3 of fibers ($f_v = 0.0048$).

Before starting the measurements, a standard SOL (Short, Open, Load) calibration is carried out, establishing the reference plane at the end of the flexible cable. Then the probe is connected to it and the reflection coefficient is measured for three reference materials. With these measurements, calibration factors are computed as with the SOL calibration [6]. These calibration factors subsequently can be used to calibrate the measurements, yielding the true reflection coefficient at the aperture of the probe. For the moderate sized probe, the inversion for the relative complex permittivity can be done with the model by Stuchly *et al.* [4].

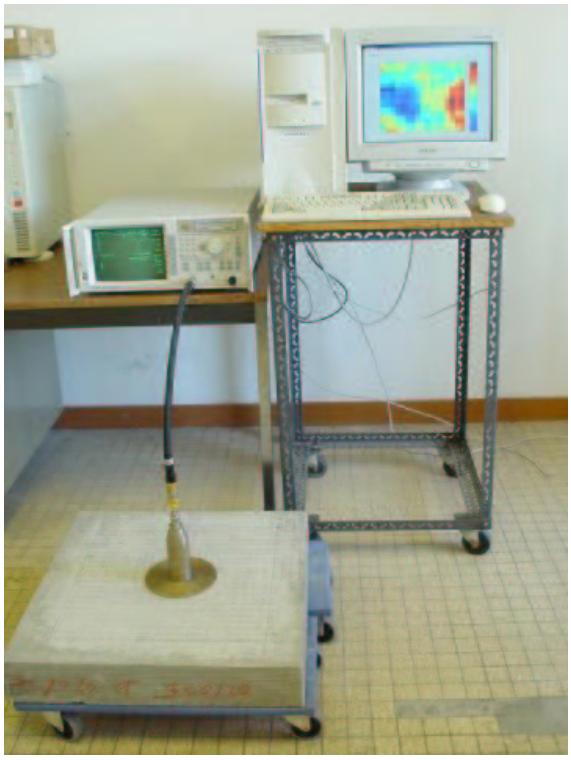

Figure 2: Moderate sized probe.

	S00	S20	S40
$\varepsilon_r^{\text{'min}}$	4.963	5.705	5.784
$\varepsilon_r^{\text{'max}}$	6.192	13.702	25.458
$\varepsilon_r^{\text{''min}}$	0.066	0.124	0.042
$\varepsilon_r^{\text{''max}}$	0.418	0.805	2.929
$<\varepsilon'_{\text{r}}>$	5.45	7.77	9.54
$<\varepsilon''_{\text{r}}>$	0.16	0.27	0.39
$\sigma_{\varepsilon'_r}$	0.20	1.65	2.66
$\sigma_{\varepsilon''_r}$	0.03	0.10	0.27

Table 1: Results for the moderate sized probe

The optimum frequency range for this probe is between 600 MHz and 1.3 GHz. We checked by means of [5] that if the thickness of the SFRC slab is at least twice the outer radius b, the slab can be considered as a half-space. The measurements on the slabs S00, S20 and S40 were done on a grid of 23 by 23 points, equally spaced 20 mm in both transverse directions. Table 1 shows for each slab the minimum and maximum complex permittivity values over the grid $\varepsilon_r^{\min}$ and $\varepsilon_r^{\max}$, the mean value $<\varepsilon_{\text{r}}>$ and the standard deviation σ_{ε_r}, at 600 MHz. The spatial variations in the permittivity of S00 are small. The mean value for S00, $\varepsilon'_{\text{r}} = 5.45$, was taken as the background permittivity $\varepsilon_{\text{r,h}}$ for deriving the fiber content of S20 and S40 with (1). The mean values for S20 and S40 are $\varepsilon'_{\text{r}} = 7.77$ and $\varepsilon'_{\text{r}} = 9.54$, respectively, and the corresponding fiber volume fractions are 18.8 kg/m^3 and 33.0 kg/m^3, respectively. The result for the smaller volume fraction (20 kg/m^3) thus is better than that for the higher volume fraction (40 kg/m^3). The measurements on S20 and S40 show larger spatial fluctuations, i.e. this probe is quite sensitive to the local distribution of the fibers. Therefore the permittivities were averaged over subspaces of about 20 by 20 cm of the grid, as explained in [2]. To avoid this averaging procedure, a larger probe was constructed.

5 MEASUREMENTS WITH A LARGE PROBE

This is a 50 Ω air-filled probe with the following parameters (Fig. 1): $a = 43$ mm, $b = 100$ mm, $F = 100$ mm, $L_1 = 305$ mm, $L_2 = 80$ mm and $\varepsilon_{\text{r,c}} = 1$. Due to mechanical constraints the outer radius was limited to maximum $b = 100$ mm. The choice for a Teflon filling was rejected for mechnical and cost reasons. The flange is now made in a square instead of a circular shape. The probe length was chosen to ensure that higher order modes are sufficiently attenuated at the probe - cable discontinuity, e.g. the amplitude of the TE_{11} mode (lowest higher order mode) is reduced to 1% over a distance of 330 mm. A picture of this probe is shown in Fig. 3. The inner conductor is supported by two thin Teflon rings, one of which is visible in the picture.

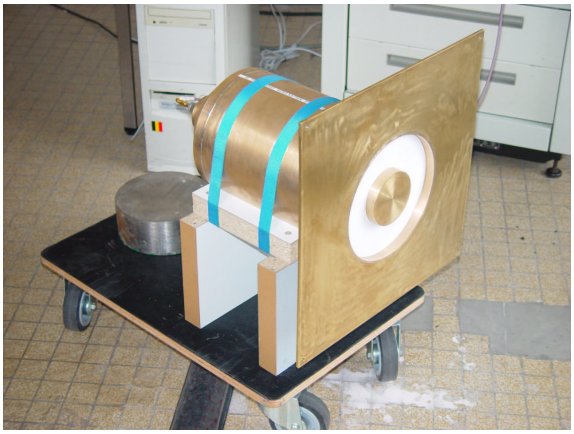

Figure 3: Large coaxial probe.

The optimum frequency range for this probe is between 100 and 400 MHz. Measurements were done on the same slabs as in the previous section. Now a grid of 4 by 4 points, equally spaced 65 mm in both transversal directions is used. Different calibrations of the probe were tested. The one-standard calibration technique yielded better results than the three standard technique. The calibrated reflection coefficient in this case is given by

$$K_{\text{cal}} = K_{\text{meas}} \frac{K^{\text{s}}_{\text{theor}}}{K^{\text{s}}_{\text{meas}}}, \qquad (2)$$

where $K^{\text{s}}_{\text{meas}}$ and K_{meas} are the measured reflection coefficients of the known calibration material and the unknown material respectively, and $K^{\text{s}}_{\text{theor}}$ is the theoretical reflection coefficient of the calibration standard. The calibration with a Teflon slab was the best. Since the thickness of the slab is less than $2b$, the inversion is done in an iterative way with the model by De Langhe *et al.* [5].

The results at a frequency of 100 MHz are shown in Table 2. The mean value for S00, $\varepsilon'_{\text{r}} = 5.24$, is taken as the background permittivity $\varepsilon_{\text{r,h}}$ for deriving the fiber content of S20 and S40 with (1). The mean values for S20 and S40 are $\varepsilon'_{\text{r}} = 7.56$ and $\varepsilon'_{\text{r}} = 10.41$, respectively, and the corresponding fiber volume fractions are 19.5 kg/m^3 and 43.3 kg/m^3, respectively. These results now are closer to the expected fiber contents than the values obtained with the moderate sized probe.

	S00	S20	S40
$\varepsilon_r^{'\min}$	5.080	6.963	9.193
$\varepsilon_r^{'\max}$	5.366	8.071	11.299
$\varepsilon_r^{''\min}$	0.149	0.179	0.276
$\varepsilon_r^{''\max}$	0.157	0.208	0.339
$<\varepsilon'_r>$	5.24	7.56	10.41
$<\varepsilon''_r>$	0.15	0.20	0.31
$\sigma_{\varepsilon'_r}$	0.09	0.32	0.51
$\sigma_{\varepsilon''_r}$	0.002	0.01	0.02

Table 2: Results for the large sized probe

Rel. variances moderate sized probe (%)			
Variance	S00	S20	S40
$\sigma_{\varepsilon'_r}$	3.65	21.23	27.89
$\sigma_{\varepsilon''_r}$	19.24	37.75	68.08
Rel. variances large probe (%)			
Variance	S00	S20	S40
$\sigma_{\varepsilon'_r}$	1.66	4.20	4.94
$\sigma_{\varepsilon''_r}$	1.69	4.20	4.93

Table 3: Comparison of the relative variances on the permittivities measured with both probes.

6 COMPARISON OF THE TWO PROBES

When comparing the results for the two different probes, the following conclusions can be drawn. The global average permittivity values over the total grids are comparable for both probes, as can be seen from Tables 1 and 2, but local spatial variations are more important with the moderate sized probe than with the large probe. The variance relative to the mean value (in %) is shown in Tabel 3. It follows that for both probes the variance grows larger with increasing fiber volume fraction. However, the variances for the larger probe are much smaller than those for the moderate sized probe. The active area of an open-eded coaxial probe roughly is given by the aperture area within the outer conductor. The active area of the large sized probe (≈ 314 cm^2) is approximately 25 times larger than that of the moderate sized probe (≈ 12 cm^2), such that there is no need to perform a spatial averaging. It is concluded that the large probe is more suited to measure the fiber content in SFRC.

7 CONCLUSIONS

Recently, a non-destructive measurement technique was introduced by the authors [2]. The technique relies on the use of an open-ended coaxial probe measurement method. In previous work, a moderate sized probe was used. This probe showed relatively large spatial variations in the measured permittivity. In this paper, a large probe was build. The results with this probe showed significantly smaller spatial permittivity variations. This is due to the larger active area of the probe. It can be concluded that this larger probe is more suited for measuring permittivities of SFRC.

Acknowledgments

This work was sponsored by the Fund for Scientific Research - Flanders. The authors are grateful to L. Haentjens for constructing the large open-ended coaxial probe.

References

[1] L. Taerwe, A. van Gysel, G. de Schutter and J. Vyncke, "Experimental determination of the steel fibre content in fresh and hardened concrete used for concrete slabs on grade," *Proceedings of the Asian-Pacific Specialty Conference on Fibre Reinforced Concrete* Ed. T.S. Lok, pp. 255–261, Aug. 1997.

[2] S. Van Damme, A. Franchois, D. De Zutter, and L. Taerwe, "Nondestructive Determination of the Steel Fiber Content in Concrete Slabs With an Open-Ended Coaxial Probe," *IEEE Trans. Geoscience Remote Sens.*, Vol. 42, pp. 2511–2521, Nov. 2004.

[3] P. De Langhe, K. Blomme, L. Martens and D. De Zutter, "Measurement of low-permittivity materials based on a spectral-domain analysis for the open-ended coaxial probe," *IEEE Trans. Instrum. Meas.*, Vol. 42, pp. 879–886, Oct. 1993.

[4] S.S. Stuchly, C.L. Sibbald and J.M. Anderson, "A new aperture admittance model for open-ended waveguides", *IEEE Trans. Microwave Theory Tech.*, Vol. 42, pp. 192–198, Feb. 1994.

[5] P. De Langhe, L. Martens and D. De Zutter, "Design Rules for an Experimental Setup Using an Open-Ended Coaxial Probe Based on Theoretical Modelling," *IEEE Trans. Instrum. Meas.*, Vol. 43, pp. 810–817, 1994.

[6] A. Kraszewski, M.A. Stuchly, and S.S. Stuchly, "ANA Calibration Method for Measurements of Dielectric Properties," *IEEE Trans. Instrum. Meas.*, Vol. 32, pp. 385–387, 1983.

PROCEEDINGS
OF JOINT

9th International Conference on Electromagnetics in Advanced Applications ICEAA '05

and

11th European Electromagnetic Structures Conference EESC '05

Under the auspices of and supported by

CITTA' DI TORINO

ICEAA '05 - 9th International Conference on Electromagnetics in Advanced Applications and EESC '05 - 11th European Electromagnetic Structures Conference

September 12-16, 2005

Torino, Italy

ISBN 88-8202-093-2